Journal of ELECTRICAL ENGINEERING, VOL. 53, NO. 9-10, 2002, 250–255

DESIGN OF A NOVEL SMA–ACTUATED ANTHROPOMORPHIC GRIPPER

Yang Kai — Gu Chenglin *

An active robot finger 10 mm in outer diameter with a shape memory alloy (SMA) wire actuator embedded to the finger with a constant distance from the geometric center of the finger was designed and fabricated. The active finger consists of two bending parts, SMA actuators, and a connecting part. The practical specifications of the SMA wire and the flexible rod were determined based on a series of formulae. The mechanical properties of the bending part are also investigated. Finally, we design a robot hand using three fingers, and the grasping experiment was carried out to prove the hand works well.

K e y w o r d s: SMA; SMA actuator; flexible rod; robot hand; grasping

1 INTRODUCTION

As control and robotic systems continue to decrease in size and weight, so must their respective component. Actuators, the driving mechanism behind these systems, play a critical role in the system design and typically rely on electric, hydraulic, or pneumatic technology.

Unfortunately, there is a drastic reduction in the power that these forms of actuation can deliver as they are scaled down in size and weight. This restriction has opened investigation of several novel actuator technologies such as those relying on piezoelectrics, polymer gels, magnetostrictive effects, electrostatics, and shape memory alloy (SMA).

Of these technologies, SMA actuators have a clear advantage in strength to weight ratio. With the high inherent strength of SMA comes the advantage of being able to implement direct drive devices. Direct drive devices eliminate the use of gears with their inherent problems of backlash and wear. Further, with the increased interest in mechatronics, SMA actuators with their silent, smooth and lifelike motions are easily adapted to miniaturization in design.

Shape memory alloy as an engineering material has been known for more than 50 years. A SMA, which is annealed at a certain temperature, can memorize the shape. When it is heated above the transition temperature, the deformed SMA can recover its original shape. We call the special ability of SMA shape memory effect (SME). Since the discovery of the shape memory effect, many materials have been found to exhibit such properties. The most common is an alloy of nickel and titanium called Nitinol (NiTi). Materials that exhibit shape memory only upon heating are referred to have one-way shape memory. Some materials also undergo a change in shape upon recooling. These materials have wo-way shape memory. Generally, the displacement and force occurred by the one-way SMA is more than that of the two-way SMA. As a representative one-way SMA actuator, Nitinol capable of up to 8.5 % strain recovery and 180 MPa stress restoration with many cycles. So, it is used very widely.

In 1984, Honma [1] demonstrated that it is possible to control the amount of actuation by electric heating, thus opening the use in robotic application. A skeleton muscle type robot was presented that consisted of a 5 degree of freedom (DOF) arm constructed of an aluminum-pipe skeleton operated with thin SMA fibers (0.2 mm) and bias springs. The end-effector of the robot was a gripper driven by a pair of antagonistic fibers. This is the earliest attempt of using SMA to the actuated robot arm. Afterward, Kuribayashi proposed an antagonistic pair of fibers for the operation of a rotary joint in 1986[2]. This is one of the most common configurations for a SMA-actuated joint, as shown in Fig. 1. The counter-clockwise motion is achieved by applying current to the top wire, causing its temperature to increase. This induces a phase change from martensite to austenite, and the resulting wire contraction. Motion in the opposite direction is produced by heating the lower wire. Examples of the use of this actuator mechanism in robotic-type applications include the inverted pendulum described by Hashimoto [3], and an inter-phalangeal actuator for robotics fingers, reported by Bergamasco [4]. A similar mechanism, which replaces one of the active wires bias spring, has been applied to a walking biped robot[3] and a robotic hand [5].

Several researchers have implemented shape memory technology for use in articulated hands. In 1984, Hitachi produced a four-fingered robotic hand that incorporated twelve groups of 0.2 mm fibers that closed the hand when activated. Dario [6] proposed an articulated finger unit using antagonistic coils and a heat pump in 1987. Gharaybeh and Burdea [7] (1995) fit several SMA springs to the Exos Dextrous Hand Master for use as a force feedback controller.

* College of Electrical and Electronics Engineering Huazhong University of Science and Technology, Wuhan, 430074, P. R. China

ISSN 1335-3632

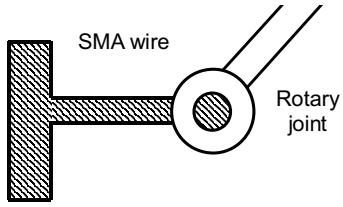

Fig. 1. Two wire rotary actuators configuration.

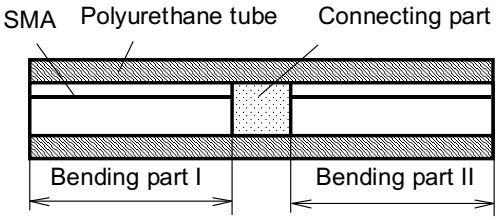

Fig. 2. Vertical section of the finger.

Among most of the designs of the robot hand using SMA, we usually see the separation between actuating elements and executing elements. So, the structure is still complex, which hampers the further use in miniature robot systems. Moreover, the cartoon motions of robot hand hamper the use in grasping and fine manipulation. To solve the problem, we present a novel robot hand.

2 STRUCTURE AND MECHANISM

2.1 Rod with embedded SMA wire actuator

Before discussing the structure of the robot hand, we investigate a cylindrical rod with a single off-axis embedded one-way SMA wire actuator. The rod is molded at temperatures below the transition temperature of the SMA actuator. SMA which is trained to shorten upon heating is embedded to the rod with a constant distance from the geometric center of the rod.

Heating of the SMA wire specimen with proper thermomechanical treatment will result in strain recovery with the ability to perform work, and, in the case of a rod embedded with axis SMA wire actuators, the contraction of the wire will cause a distributed force to act upon the rod. Since the actuator is not located on the neutral axis of the rod, the actuation force also results in a moment which causes the rod to bend. Upon cooling, the SMA actuators are stretched out by the flexible rod through an interfacial shear, the finger returns to a straight shape. So this constructs the two-way reversible actuating elements.

2.2 Finger

In order to increase the bending angle of the finger, and to perform smooth anthropomorphic grasping, upon the elicitation of the structure of the human hands, we propose a novel robot finger with multi-units, as shown in Fig. 2. The finger has two flexible rods 8 mm in diameter with embedded SMA wires 0.5 mm in diameter, one shorter rod as a connecting part. All the parts are covered with a polyurethane tube 10 mm in outside diameter. On both sides of each SMA wire, there are guiding wires. All the guiding wires are covered under the tube to ensure the structure compact. In the base of the design of fingers, we design a prototype of a three-fingered hand as shown in Fig. 9. By the joule heat from a special supply, the temperature of the SMA actuators achieves the transformation temperature easily, resulting in the anthropomorphic, flexible, three-dimensional motion of the novel gripper. Once stopping heating the SMA actuators, the hand returns to its initial relaxed shape as soon as the temperature of SMA actuators falls down.

3 DESIGN AND FABRICATION

3.1. Physical model of SMA

As we know, SME depends on the reversible transformation between two crystalline phases known as austenite (at high temperature) and martensite. The transformation is observed by noting the volume fraction of martensite ξ, which can vary between 0 (all austenite) and 1 (all martensite). In our design, we adopt the cosine model [8] which relates the SMA martensite volume fraction to temperature T and stress σ, the transformation from martensite to austenite is defined by:

$$\xi(\sigma,t) = \frac{1}{2}\Big(\cos\big[a^M(T - M_f^0) - \frac{a^M}{c^M}\sigma\big] + 1\Big)\,. \quad (1)$$

While the transformation from austenite to martensite is defined by:

$$\xi(\sigma,t) = \frac{1}{2}\Big(\cos\big[a^A(T - A_s^0) - \frac{a^A}{c^A}\sigma\big] + 1\Big)\,. \quad (2)$$

The constants c^A and c^M are the linear relationships between the stress and the SMA transition temperatures, while a^A and a^M represent constants of the model which provide for the volume fraction to be either 0 or 1 at the end of transformation.

Upon being heated by an appropriate supply, the temperature of the SMA actuator is changed incrementally. Since the SMA material properties change with the martensite volume fraction according to the rule of mixtures, the actuation force imparted by the actuator will depend upon the temperature and stress state of the SMA. Using the theory of mixtures, we approximately estimate the Young modulus of the SMA as follows:

$$E^a = \xi E^M + (1 - \xi)E^A\,. \quad (3)$$

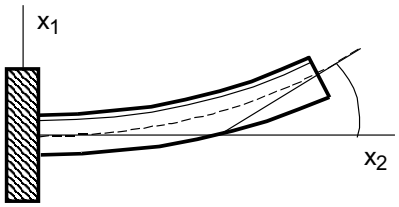

Fig. 3. Configuration of the rod.

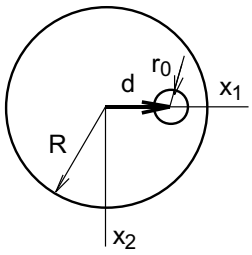

Fig. 4. Cross section of the rod.

Here E^M is the Young modulus of the SMA in the martensite phase and E^A is in the austenite phase. In terms of other material properties such as the coefficient of thermal expansion, since the difference between the value in martensite phase and austenite phase is slight, we can use the average values to estimate the variables during transformation as follows:

$$\alpha = \left(\alpha^A + \alpha^M\right)/2\,. \tag{4}$$

Here α^A and α^M are the coefficients of thermal expansion in austenite phase and martensite phase.

With the definition of the material properties, the thermo-mechanical response of the SMA can be described by a constitutive law and a flow rule.

$$\sigma = E^a\varepsilon^e = E^a\left(\varepsilon - \varepsilon^t - \alpha(T - T_0)\right), \tag{5}$$

$$\varepsilon^t = \Lambda\dot{\xi}\,. \tag{6}$$

The coefficient of linear thermal expansion α, the SMA transformation strain ε^t and variable Λ provide sensing of direction to the flow rule.

3.2. Parametric design of the active rod

The theory of flexible rods with embedded line actuators has been developed by Lagoudas and Tafjbakhsh [9] to account for the deformations of elastomeric rods with SMA actuators envisioned for shape control applications. Our robot finger is a specific case of plane deformations of a rod, as shown in Fig. 3 and Fig. 4. The equilibrium equation of the rod reduces in this case to the set of three Eqs. (7)–(9) for the shear force F_1, axial force F_3, and bending moment M_2.

$$\frac{\mathrm{d}F_1}{\mathrm{d}s} + k_2(F_3 + F^a) = 0\,, \tag{7}$$

$$\frac{\mathrm{d}F_3}{\mathrm{d}s} - k_2F_1 + \frac{\mathrm{d}F^a}{\mathrm{d}s} = 0\,, \tag{8}$$

$$\frac{\mathrm{d}M_2}{\mathrm{d}s} + (1+e)F_1 - d^a\frac{\mathrm{d}F^a}{\mathrm{d}s} = 0\,. \tag{9}$$

The constitutive equation for the rod are assumed to be:

$$M_2 = EI_2k_2\,, \tag{10}$$

$$F_3 = AEe + EI_2k_2^2 \approx EAe \tag{11}$$

The constitutive equation for the line actuator is approximated by the following:

$$F^a = A^a\sigma^a = A^aE^a[e - k_2d - \varepsilon^t\alpha^a(T - T_0)]\,. \tag{12}$$

Here k_2 is the bending curvature, e is the elongation of the rod, and F^a is the actuation force of the SMA wire, E^a, E are Young's moduli of the line actuator and rod, and A^a, A are their cross-sections, respectively, I_2 is the moment of inertia of the cross-section of the rod. The distance of the actuator form the axis of the rod is denoted by d.

Since the average shear stress on the cross section of the rod has insignificant effects upon the elastomer [10], an approximation $F_1 = 0$ may be introduced to simplify the solution.

The expressions from Lagoudas and Tadjbakhsh are now revisited. The rod equations can be simplified to:

$$F_3 + F^a = 0\,,$$

$$M_2 - F^ad = 0\,.$$

After substituting the constitutive equations into Eqs. (13)–(14), the curvature is found to have the following expression:

$$k_2 = \frac{\alpha\beta d}{1 + \beta(1 + \alpha d^2)}[\varepsilon^t + \alpha^a(T - T_0)]\,. \tag{15}$$

Elongation e of the centroidal line of the rod is given by:

$$e = \frac{\beta}{1 + \beta(1 + \alpha d^2)}[\varepsilon^t + \alpha^a(T - T_0)]\,. \tag{16}$$

The constants are defined as $\alpha = A/I_2$ and $\beta = E^aA^a/EA$. The deformation of the rod is then calculated in terms of the curvature k_2, *ie*:

$$k_2 = \frac{\mathrm{d}\theta}{\mathrm{d}s}\,, \tag{17}$$

$$u_1 = \int_0^s (1+e)\sin\theta\mathrm{d}s + u_1(0)\,, \tag{18}$$

$$u_3 = \int_0^s (1+e)\cos\theta\mathrm{d}s + u_3(0)\,. \tag{19}$$

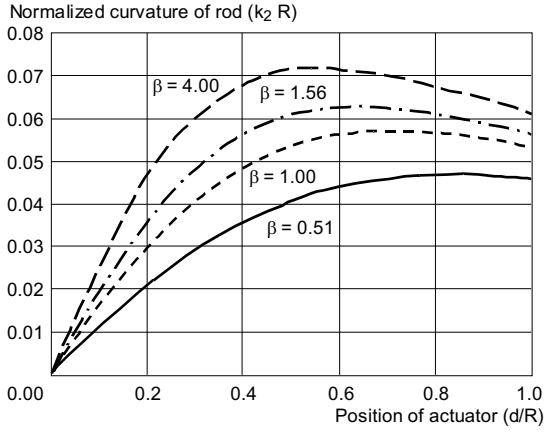

Fig. 5. Maximum deflection of the rod versus the normalized position of the actuator.

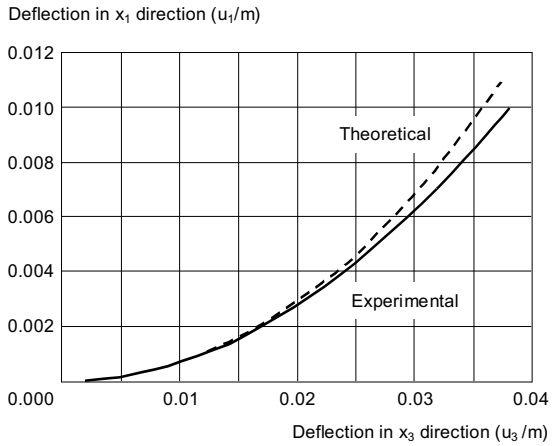

Fig. 6. Deflection of the rod.

For our active finger, the boundary conditions are $u_1(0) = u_3(0) = 0$. Since k_2 is constant, the deflections u_1 and u_3 can be explicitly integrated:

$$u_1(s) = \frac{1+e}{k_2}(1 - \cos k_2 s)\,, \tag{20}$$

$$u_3(s) = \frac{1+e}{k_2} - \sin(k_2 s)\,. \tag{21}$$

Figure 5 is the curve of the normalized curvature, $k_2 R$, versus the normalized distance, d/k_2, of the actuation wire to the centroid of the rod. It is interesting to see that the curvature, k_2, is not always increasing monotonically with increasing distance d. The reason is that the actuator is a strain actuator. Although it can generate a larger moment for a given amount of actuation force if placed further away from the center of the rod, it also relaxes more by bending. Thus the total actuation effect may be less. The optimal distance depends on the ratio β.

Figure 6 presents a comparison of the theoretical prediction with experimental data. The geometry and material data of the rod are $r_0 = 0.25$ mm, $R = 8$ mm, $\varepsilon^{\max} = 0.08$, $l = 40$ mm, $E^A = 120$ GPa, $E^M = 50$ GPa. The maximum displacement error in x_1 direction is about 1.5 mm.

$$\begin{aligned} X_e &= \frac{l_1 \sin 2\theta_1}{2\theta_1} + l_2 \cos 2\theta_1 + \frac{l_3(\sin\theta_3)\cos(2\theta_1+\theta_3)}{\theta_3}, \\ Y_e &= \frac{l_1(1-\cos 2\theta_1)}{2\theta_1} + I_2 \sin 2\theta_1 + \frac{l_3(\sin\theta_3)\sin(2\theta_1+\theta_3)}{\theta_3}, \end{aligned} \tag{22}$$

$$Orientation = \theta = 2(\theta_1 + \theta_3)\,, \tag{23}$$

$$\begin{aligned} Transmatrix &= Trans(X_e, Y_e, 0) Rot(Z, \theta) \\ &= \begin{bmatrix} \cos\theta & -\sin\theta & 0 & X_e \\ \sin\theta & \cos\theta & 0 & Y_e \\ 0 & 0 & 1 & 0 \\ 0 & 0 & 0 & 1 \end{bmatrix} \end{aligned} \tag{24}$$

3.3. Model of finger

To control the position and orientation of the fingertip of the finger the relationship between the end positions of one finger should be known. The homogeneous transformation matrix which express the position and orientation of the ends of a finger will be derived. Figure 7 shows the geometrical relations between the two ends of the finger taking one of the ends at origin. From this figure, the coordinate of the end of the finger is expressed as (X_e, Y_e) and the orientation of the tangent direction of the ends is θ, therefore, the homogeneous transformation matrix of the end can be derived as equations Eqs. (22)–(24).

3.4 Fabrication of the finger

3.4.1 Preparation of the SMA actuators

The SMA wire, produced in the Chinese Academy of Science, was received in a coil. In order to insure the actuators to have a perfectly straight memory shape, it was decided to anneal the SMA while clamped in a straight configuration.

Once annealed, the SMA actuators must be carefully strained by the desired amount. To achieve these ends, a unique annealing and straining jig was designed and fabricated of steel. This jig was designed to clamp the SMA in a straight configuration and to be heated in a furnace or used to stretch the SMA wire.

The following protocol was used to prepare SMA actuators:

1) The SMA wire was cut into 5 cm lengths and clamped into the jig.
2) Annealed at 500 °C for 1/2 hour in the local steel treater's furnace.
3) Dip in water at room temperature to cool down the SMA actuators.
4) Strain SMA actuators by stretching and measuring twinned deformation.

Table 1. The specifications of used SMA wire actuator

1) Composition	Ti-50.2 at% Ni	6) Density	6.5gm/cc
2) Annealing condition	500 °C 1/2 hour	7) Thermal Conductivity	0.209w/cm °C
3) Dimension	$\phi 0.5 \times 40$ mm	8) Coef. of Thermal Expansion	8.5×10^{-6} °C
4) Maximum strain	0.08	9) Specific Heat	6–8Cal/mol °C
5) Young's modulus A : Austenite M : Martenite	A : 120Gpa M: 50Gpa	10) TransformationTemperatures(°C)	$M_s = 65,\ M_f = 15,$ $A_s = 26,\ A_f = 80$

Table 2. Specifications of the produced 3 segment active robot finger

1) Dimension	ϕ80 mm	5) Maximum Open Loop Duty Ratio	48 %
2) Maximum Bending Angle	60degree	6) Internal Diameter of the Tube	8 mm
3) Power Source	4 v	7) Outside Diameter of the Tube	10 mm
4) Maximum Closed Loop Duty Ratio	80 %	8) Length of Connecting Part	10 mm

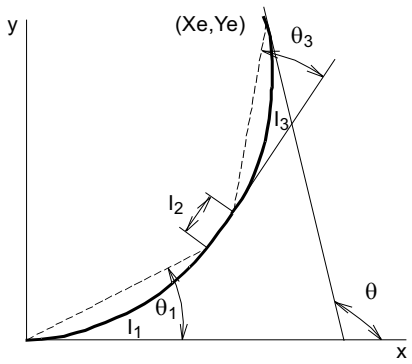

Fig. 7. Coordinates system of the finger.

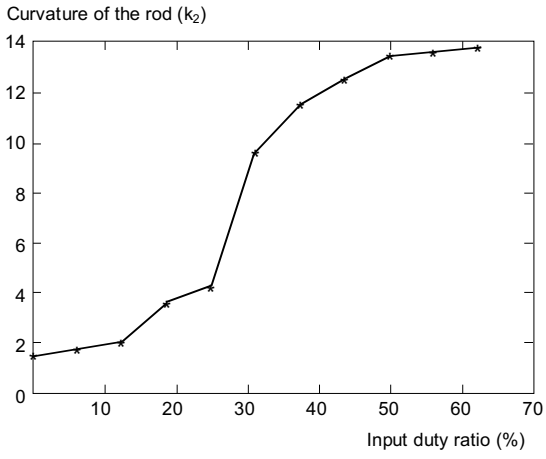

Fig. 8. Relationship between the duty ratio and curvature of the rod.

Specifications of the SMA actuator used in the active robot finger are summarized in Table 1.

3.4.2 Preparation of an active flexible rod with embedded SMA actuator

A review of thermoset and thermoplastic polymers revealed a few thermoset polymers that would satisfy the stiffness and room molding compounds, silicone molding compounds, and some epoxy foumulations. It was found that although the polyurethane is know to bond to metal better than the silicone, under conditions of a heated SMA actuators, the polyurethane debonded. So, it was decided to design the active rod using the silicone mold making compound. The materials we adopt is called RTV (Room Temperature Vulcanization) silicone rubber 515. To prepare this rod, a special mold was constructed that could easily come apart for demolding. The SMA actuators were sandblasted, strained and clamped into the mold. Subsequently, as the fabrication of the rod, we mold a 10 mm length connecting part. After placing the guiding wire at both ends of one rod, we connected the two rod with the connecting part and cover the bending parts and connecting part in the polyurethane tube, the specifications of fingers are summarized in Table 2.

Finally, three fingers were fixed at the vertex of the equilateral triangle to complete anthropomorphic grasping as shown in Fig. 9.

4 DRIVING EXPERIMENT

The relation between the duty ratio and curvature of the rod is shown in Fig. 8. It is assumed that the polyurethane tube is flexible enough to have a slight effect on the bending of the rod. The curvature was constant to approximately 3.8, and thereafter the curvature rose rapidly. The curvature was about 14 when the duty ratio was 48 %. The open loop maximum duty ratio is about 48 %. Considering handling feedback resistance values of the SMA wire actuator, the closed loop maximum duty ratio is about 80 %.

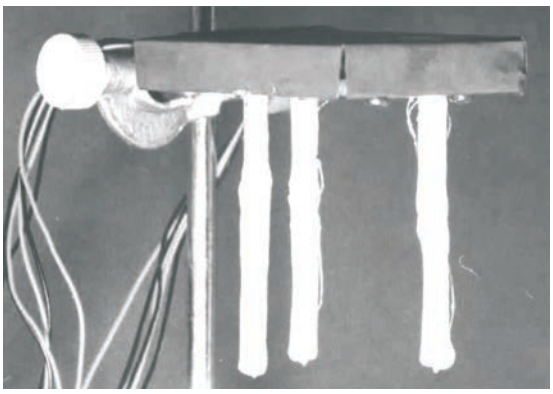

Fig. 9. Configuration of hand without activating.

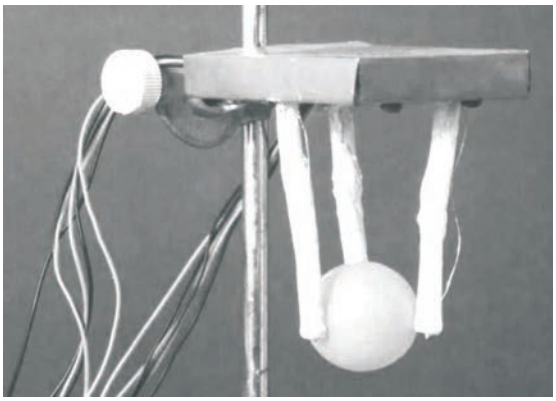

Fig. 10. Grasping sphere.

To verity the basic performance of the robot hand, the driving experiment was conducted to grasp a sphere with a weight of 3 N and radius 15 mm, as shown in Fig. 10. The novel hand proved to make pliable motion with about 40 (deg/sec) up to the designed maximum angle (60 deg) at the responding speed high enough for the purpose. By controlling the bending of each finger, the hand can accomplish fine manipulation like human hands.

5 CONCLUSION

We develop the theory of flexible rods with embedded line actuators. An active rod of 8 mm in outer diameter with SMA wire actuators was design and fabricated. Using the rods, we designed a three-fingered robot gripper to accomplish anthropomorphic grasping and fine manipulations. The maximum bending angle of the finger was about 60 degrees when the duty ratio is 48 %. The prototype can grasp a sphere of 15 mm in radius. The motions are flexible and lifelike. A clear picture of the grasping experiment shows that the fingertip could reach the set point fast and precisely.

Acknowledgements

The authors acknowledge the Shenyang Institute of Metals of the Chinese Academy of Science for supplying the NiTi SMA wires. They also acknowledge many useful discussions with Chenguang Institute of Chemical Engineering.

References

[1] DAI HONMA—YOSHIYUKI MIWA—NOBUHIRO IGUCHI: Micro Robots and Micro Mechanisms Using Shape Memory Alloy, In Integrated Micro Motion Systems, Micro-machining, Control and Application. Nissin. Aichi. Japan. Oct. 1989. The Third Toyata conference.

[2] KURIBAYASHI, K.: A New Actuator of a Joint Mechanism Using TiNi Alloy Wire, The Int. Journal of Robotics Research **4** No. 4 (1986).

[3] MINORU HASHIMOTO—MASANORI TAKEDA—HIROFUMI SAGAWA—ICHIRO CHIBA—KIMIKO SATO: Application of Shape Memory Alloy to Robotic Actuators, Robotic Systems **2** No. 1 (1985), 3–25.

[4] M. BERGAMASCO, F. SALSEDO—P. DARIO.: A Linear SMA Motor as Direct-Drive Robotic Actuator, IEEE International Conference on Robotics and Automation (1989) pp. 618–623.

[5] NAKANO, Y.—FUJIE, M.—HOSADA, Y.: Hitachi's Robot Hand, Robotics Age **6** No. 7 (1984), 18–20.

[6] DARIO, P.—BERGAMASCO, M.—BERNARDI, L.—BICCHI, A.: A Shape Memory Alloy Actuating Module for Fine Manipulation, In IEEE Micro Robots and Teleoperator Workshop, Hyannis, Ma, Nov 9–11 1987. IEEE Robotics and Automation council.

[7] GHARAYBEH, M. A.—BURDEA, G. C.: Investigation of a Shape Memory Alloy Actuator for Dextrous Force-Feedback Masters, Advanced Robotics **9** No. 3 (1995), 317–329.

[8] LAGOUDAS, D. C.—TADJBAKHSH, I. G.: Deformation of Active Flexible Rods with Embedded Line Actuators, Smart Mater. Struct **2** (1993), 71–81.

[9] LAGOUDAS, D. C.—TADJBAKHSH, J. G.: Active Flexible Rods with Embedded SMA Fibers, Smart Mater. Struct **1** (1992), 162–167.

[10] LAGOUDAS, D. C.—BO, Z.—QIDWAI, M. A.: A Unified Thermodynamic Constitutive Model for SMA and Finite Element Analysis of Active Metal Matrix Composites, Mech. Composite Mater. Struct. **4** (1996), 153–179.

Received 5 April 2002

Yang Kai, A postgraduate student of the College of Electrical and Electronics Engineering at Huazhong University of Science and Technology, Wuhan, 430074, China. He was born in 1976 and obtained his Bachelor's Degree of Engineering from HUST in June 1998. His research field are shape memory alloy actuators and their control systems.

Gu Chenglin, Professor, College of Electrical and Electronics Engineering at Huazhong University of Science and Technology, Wuhan, 430074, China. He was born in 1954. He obtained his Doctor's Degree from HUST in 1989. He is a Founder Member of ICS, a member of IEE, Ceng. His research field are novel motors and their control systems.